Efficient preparation of highly pure chlorin e_6 and its photodynamic anti-cancer activity in a rat tumor model

YEON-HEE MOON[1], SEONG-MIN KWON[1], HYO-JUN KIM[2], KWAN-YOUNG JUNG[2], JONG-HWAN PARK[1], SOO-A KIM[3], YONG-CHUL KIM[2], SANG-GUN AHN[1] and JUNG-HOON YOON[1]

[1]Department of Pathology, School of Dentistry, Chosun University, Gwangju 500-759; [2]Department of Life Science, GIST, Gwangju 500-715; [3]Department of Biochemisry, College of Oriental Medicine, Dongguk University, Gyungju 780-714, Korea

Received May 28, 2009; Accepted July 24, 2009

DOI: 10.3892/or_00000540

Abstract. Photodynamic therapy (PDT) is currently being used as an alternative therapeutic modality for a variety of malignant tumors. This study was performed to show an efficient preparation of second generation of photosensitizer chlorin e_6 (Ce_6) with high yield and purity, and to test antitumor activity of Ce_6-induced PDT (Ce_6-PDT) both *in vitro* and *in vivo* using a rat tumor model. Three-week-old male Sprague-Dawley (SD) rats were inoculated s.c. on the right flank with $5x10^6$ RK3E-ras cells. The animals were administered i.v. with Ce_6 (10 mg/kg) and 24 h later, PDT was performed using a laser diode at a light dose of 100 J/cm^2. Ce_6-PDT generated reactive oxygen species and led to significant growth inhibition in RK3E-ras cell. In addition, Ce_6-PDT induced apoptosis through the activation of caspase-3 and its downstream target, PARP cleavage. The protein level of anti-apoptotic bcl-2 was also reduced by Ce_6-PDT in RK3E-ras cells. In *in vivo* experiments, application of Ce_6-PDT led to a significant reduction of tumor size. PCNA immunostaining and TUNEL assay revealed that Ce_6-PDT inhibited tumor cell proliferation and increased apoptosis. These findings suggest that the newly purified Ce_6-PDT can effectively arrest tumor growth by inhibiting cell proliferation and inducing apoptosis.

Correspondence to: Dr Sang-Gun Ahn or Dr Jung-Hoon Yoon, Department of Pathology, School of Dentistry, Chosun University, 501-759, #375 Seosuk-dong, Dong-gu, Gwangju 501-759, Korea
E-mail: ahnsg@chosun.ac.kr or jhyoon@chosun.ac.kr

Abbreviation: PDT, Photodynamic therapy; Ce_6, chlorin e_6; SD, Sprague-Dawley; ROS, reactive oxygen species

Key words: chlorin e6, photosensitizer, photodynamic therapy, *in vivo* study, apoptosis

Introduction

Photodynamic therapy (PDT) is currently being used as a therapeutic alternative for a variety of malignant tumors. Compared with ionizing radiation therapy or chemotherapy, PDT is generally safer for the surrounding normal tissues because photosensitizers are preferentially accumulated in tumor cells (1). PDT involves the selective uptake and retention of a photosensitizer in the tumor followed by light irradiation of an appropriate wavelength to cause the destruction of tumor cells by the formation of cytotoxic reactive oxygen species (ROS) (1,2). The type I radicals including superoxide anion ($O_2^{\bullet}$), hydrogen peroxide (H_2O_2), hydroxyl radical (.OH), and type II ROS such as singlet oxygen have been implicated in the therapeutic or toxic responses of PDT (3). PDT produces cytotoxic effects through photodamage to subcellular organelles and molecules such as mitochondria, lysosomes, cell membranes, and nuclei of tumor cells, which are considered as potential targets. During light exposure, photosensitizers that are localized in mitochondria may induce apoptosis, while those localized in lysosomes and cell membranes may cause necrosis. Apoptosis is responsible for PDT-mediated tumor cell death *in vitro* and tumor ablation *in vivo* (2,4).

In clinical PDT, photosensitizers such as hematoporphyrin derivatives, Photofrin, Photosens, Levulan and Visudyne have been used exclusively. These compounds have low localization in tumors, resulting in low photodynamic effect and high skin photosensitivity (2,5). Therefore, development of compounds with higher selective affinity for tumors was required and consequently, chlorin e_6 (Ce_6) was developed as a second generation photosensitizer. It is a promising photosensitizer as it exhibits advantageous photophysical properties for PDT such as having long lifetimes in their photoexcited triplet states and high molar absorption in the red region of the visible spectrum. Moreover, a 664-nm laser light can penetrate tissue deeper that the 630-nm laser light used for Photofrin (6). However, a mixed form of Ce_6 derivatives has been prepared in the clinical application (7,8). Therefore, a standard process for the preparation of pure form of Ce_6 with high yield is required.

In this study, we developed an efficient preparation of Ce_6 with high yield and purity from chlorophyll *a* of a seawater live chlorella *(Chlorella ellipsoidea)* belonging to green algae. We investigated anticancer effect of PDT with the newly isolated Ce_6 through both *in vitro* and *in vivo* experiments.

Materials and methods

Preparation of chlorin e_6. Live chlorella *(Chlorella ellipsoidea)* 100 g (dried weight) was sequentially washed with 500 ml of water and 300 ml of 50% ethanol in water to remove polar materials and the residue was extracted twice with 500 ml of 100% ethanol to obtain chlorophyll *a* rich fraction (extraction yield 4.3%). Stirring the combined ethanol solution of chlorophyll *a* in 1 N HCl (pH 2.5) for 3 h at room temperature afforded pheophytin in the form of precipitates. The precipitate was dissolved in dichloromethane washed with distilled water, dried with anhydrous sodium sulfate, and rotary-evaporated to dryness. The residue was purified by a chromatography using neutral alumina (Aldrich, Brockmann, ~150 mesh) with a gradient elution from 30% dichloromethane in n-hexane to 100% dichloromethane. The main green band was collected and evaporated to dryness. The crystalline powder was dissolved in acetone, adjusted pH 12.0 with 1 N NaOH, and stirred for 12 h. The precipitated Ce_6 was filtered, washed with acetone and dissolved in 100 ml of water, and filtered to remove insoluble impurity. After lyophilization of the filtered water solution, a fine black powder of Ce_6 was obtained. The purity of Ce_6 is 93-98% (yield of Ce_6: 1% from dried weight of chlorella).

Cell culture. RK3E-ras cells, rat kidney epithelial cells transformed with K-ras gene, were maintained in DMEM medium containing 5% fetal bovine serum, 100 U/ml penicillin-streptomycin (Invitrogen, CA, USA) and subsequently incubated at 37˚C in an atmosphere containing 5% CO_2. RK3E-ras cells were kindly provided by Dr Eric Fearon (University of Michigan Medical School, Ann Arbor, MI) and were described previously (9).

In vitro photodynamic treatment. RK3E-ras cells ($2x10^4$ cells/well) were cultured overnight in 12-well plates and treated with different doses of Ce_6 for 24 h. Subsequently, PDT was performed using a laser diode (Geumgwang Co., Ltd., Daejeon, Korea) at a wavelength of 664 nm. The total laser energy density was 10 J/cm^2.

MTT assay. After Ce_6-PDT, the viability of RK3E-ras cells was assessed by MTT assay. Each well was washed twice with PBS, and 0.5 ml of cell culture medium and 50 μl of 3-(4,5-dimethylthiazol-2-yl)-3-5-diphenyltetrazolium bromide solution (5 mg/ml in PBS) were added. After 3 h of incubation, medium was removed and 250 μl of acid-isopropanol (0.04 mol/l HCl in isopropanol) was added. The absorbance was measured at 595 nm of microplate autoreader ELISA (Bio-Tek Instruments Inc., Winooski, VT) and all experiments were performed in triplicate.

ROS assay. After Ce_6-PDT, the cells were washed twice with PBS and incubated in medium containing 10 μM of 2'7'-dichlorofluorescein diacetate, H_2DCFDA (Molecular Probes™, Eugene, Oregon) at 37˚C in an atmosphere containing 5% CO_2 for 30 min. Fluorescence was analyzed immediately by Thermo Scientific Varioskan® Flash spectral scanning multimode reader (Varioskan, Thermo Electron Co., Waltham, MA, USA) with SkanIt® software (wavelength: excitation 450-495, emission 517-527).

Flow cytometry. At 24 h after Ce_6-PDT, $1x10^6$ RK3E-ras cells were stained to the Vybrant® apoptosis assay kit (Molecular Proves), followed by labeling Alexa Fluor® 488 Annexin V and propidium iodide. Cells (10,000) per sample were analyzed immediately using Cell Llab Quanta™ SC flow cytometer (Beckman Coulter Inc., Miami, FL) and software.

Measurement of caspase-3 activity. Activity of caspase-3 in the cells with Ce_6-PDT was measured using ApoAlert Caspase colorimetric assay kit according to the manufacturer's instructions (Clontech Laboratories, Mountain View, CA). The absorbance of the solution was measured at 405 nm using Microplate Autoreader ELISA (Bio-Tek Instruments Inc., Winooski, VT) and all experiments were performed in triplicate.

Western blotting. At 24 h after Ce_6-PDT, the cells were lysed in 1X reporter lysis buffer (Promega, Madison, WI). The total protein was resolved by 12% SDS-PAGE and transferred onto PVDF membranes. After blocking in TBS-T (20 mmol/l Tris, 137 mmol/l NaCl, 1 g/l Tween-20, pH 7.6) with 5% skim milk for 4 h at room temperature, the membranes were incubated with primary antibodies against cleaved PARP (Cell Signaling Technology, Beverly, MA), bcl-2, and actin (Santa Cruz Biotechnology, Santa Cruz, CA) for 2 h. The membranes were then washed 3 times with TBS-T and incubated with secondary antibodies for 1 h at room temperature. Finally, the membranes were visualized using the ECL detection reagent.

In vivo experiment. RK3E-ras-Fluc cells were used for *in vivo* experiment, which was previously established in our laboratory (10). Three-week-old male SD rats (Samtaco, Osan, South Korea) were inoculated s.c. on the right flank with $5x10^6$ of RK3E-ras-Fluc cells. One week later, by which time the tumors had reached ~0.7-1.0 cm in diameter, the animals were administered i.v. with Ce_6 at a dosage of 10 mg/kg. After 24 h, PDT was performed using a laser diode at a light dose of 100 J/cm^2 and wavelength of 664 nm. The animals were monitored daily and tumor volume was measured by caliper and calculated by the formula as previously described (11): $V=(ab^2)/2$, in which *a* is the longest diameter and *b* is the shortest diameter of the tumor. All experiments were performed under protocols approved by the Animal Care and Use Committee at Chosun University School of Dentistry.

Imaging. Radiographs were performed using a soft X-ray apparatus (Softex Model CMBW-2, Tokyo, Japan) with exposure of 30 sec with 25 kV and 20 mA conditions as previously described (10).

For bioluminescence imaging, the animals were anesthetized with the combination of ketamine (50 mg/kg) and xylazine (5 mg/kg) and then given i.p. with luciferin

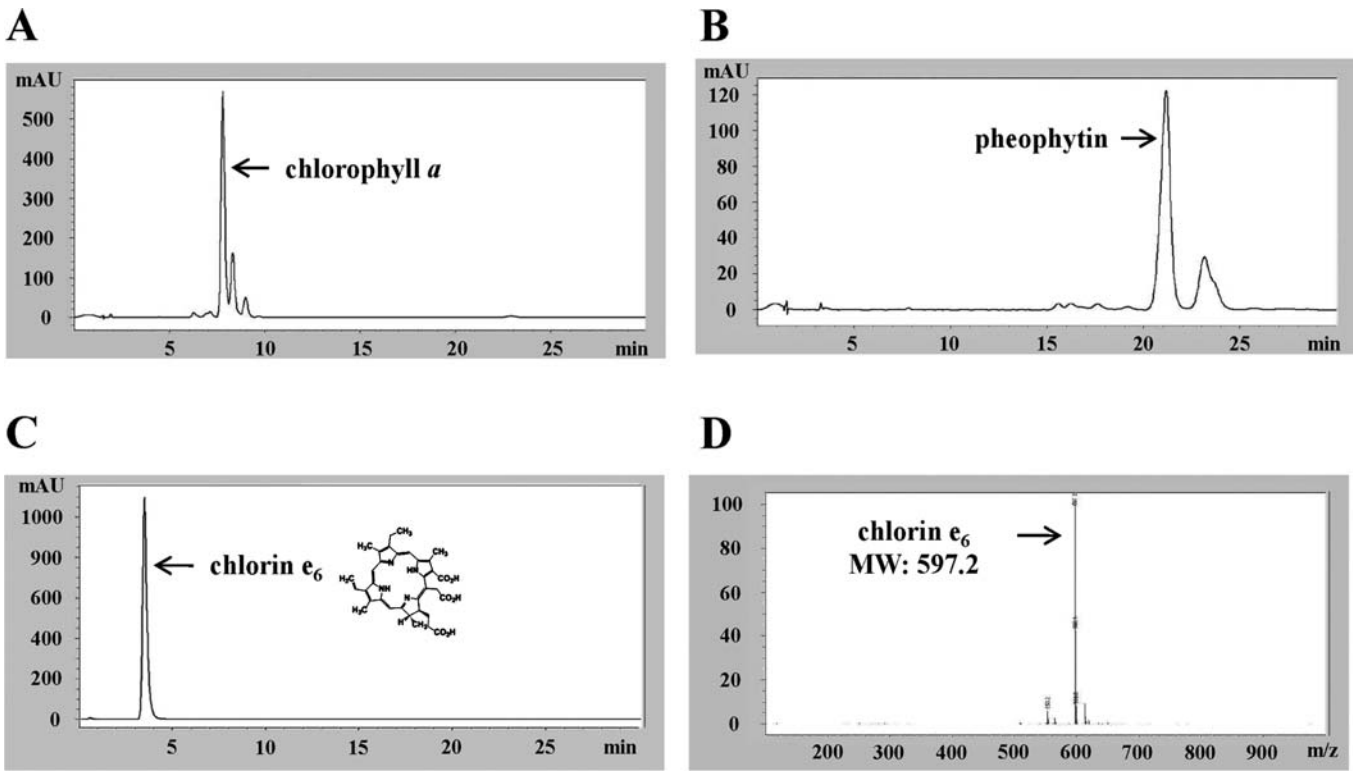

Figure 1. HPLC chromatograms and mass spectrometry of purified chlorophyll *a*, pheophytin, and chlorine e_6. (A) Chromatogram of purified chlorophyll *a* on a reverse-phase HPLC column. Separation condition is 0.1% TFA in H_2O: CH_3CN = 50:50 as an eluent for 40 min with flow rate=1 ml/min. (B) Chromatogram of purified pheophytin on a reverse-phase HPLC column. Separation condition is MeOH/ dichloromethane/ water = 62.5/ 23.5/ 0.5 as an isocratic eluent for 40 min with flow rate=1 ml/min. (C) Chromatogram of purified chlorine e_6 on a reverse-phase HPLC column. Separation condition is 0.1% TFA in H_2O: CH_3CN = 50:50 as an eluent for 40 min with flow rate=1 ml/min. (D) Mass data of chlorin e_6 was obtained from LC-MS (ESI) system.

(Molecular Probes, Palo Alto, CA) at a dose of 80 mg/kg body. The animals were imaged with the Xenogen IVIS imaging system (Xenogen Co., Alameda, CA) to record the bioluminescent signal emitted from the tumor. The IVIS-100 equipped with CCD camera system was used for emitted light acquisition, and Living Image software (Xenogen) was used for data analysis.

Histopathology, immunohistochemistry, and TUNEL assay. The animals were sacrificed on day 15 and the tumors were removed carefully and fixed in 10% formalin over 24 h. The tissues were then dehydrated in an alcohol-xylene series and embedded in paraffin wax. From each block, sections 2 μm thick were prepared and stained with haematoxylin and eosin for histological examination. For immunohistochemistry, the sections were incubated in 3% H_2O_2 in methanol for 10 min to remove endogenous peroxidase and blocked with 1% BSA in PBS for 1 h. The sections were then incubated with anti-PCNA antibody (Dako) overnight at 4˚C. After washed 3 times with PBS-T, the sections were subjected to avidin-biotin peroxidase complex (ABC) method (Vector) and peroxidase activity was evaluated with 3,3'-diaminobenzidine (Vector). Finally, the sections were counterstained with hematoxylin. The PCNA-positive cells were counted from 5 randomly selected areas under x200 magnifications and represented as mean ± SD.

The terminal deoxynucleotidyl transferase-mediated dUTP nick end-labeling (TUNEL) assay was done using an Apoptosis detection kit (Intergen, Purchase, NY) according to the manufacturer's protocol.

Statistical analysis. The differences in mean values among groups were tested, and the values were expressed as mean ± SD. All of the statistical calculations were carried out using Microsoft Excel.

Results and Discussion

The yield of chlorophyll *a* extracted from undisrupted chlorella cells with ethanol was 10 times more than that from a commercially available chlorella powder (data not shown). The retention time of chlorophyll *a* in HPLC system was 7.8 min (Fig. 1A). Treatment of the ethanol to chlorophyll *a* in an acidic condition (1 N HCl, pH 2.5) enable to remove the Mg^{2+} ion easily to afford a crude pheophytin in the form of precipitates, which could be further purified with alumina column chromatography (Fig. 1B). As the final step, pheophytin was hydrolized by reacting with 1 N NaOH (pH 12.0) to give Ce_6 as a fine powder which is a water soluble sodium salt form with 95-98% purity (Fig. 1C). The molecular weight of Ce_6 (596.2) was confirmed by an observation of 597.2 in LC-MS analysis as the $(M+H)^+$ form (Fig. 1D). The total yield of Ce_6 is 1%, based on the calculation as a percentage of obtained Ce_6 weights to the dried weight of chlorella. In this study, we established an efficient isolated procedure of highly pure Ce_6 utilizing undisrupted live

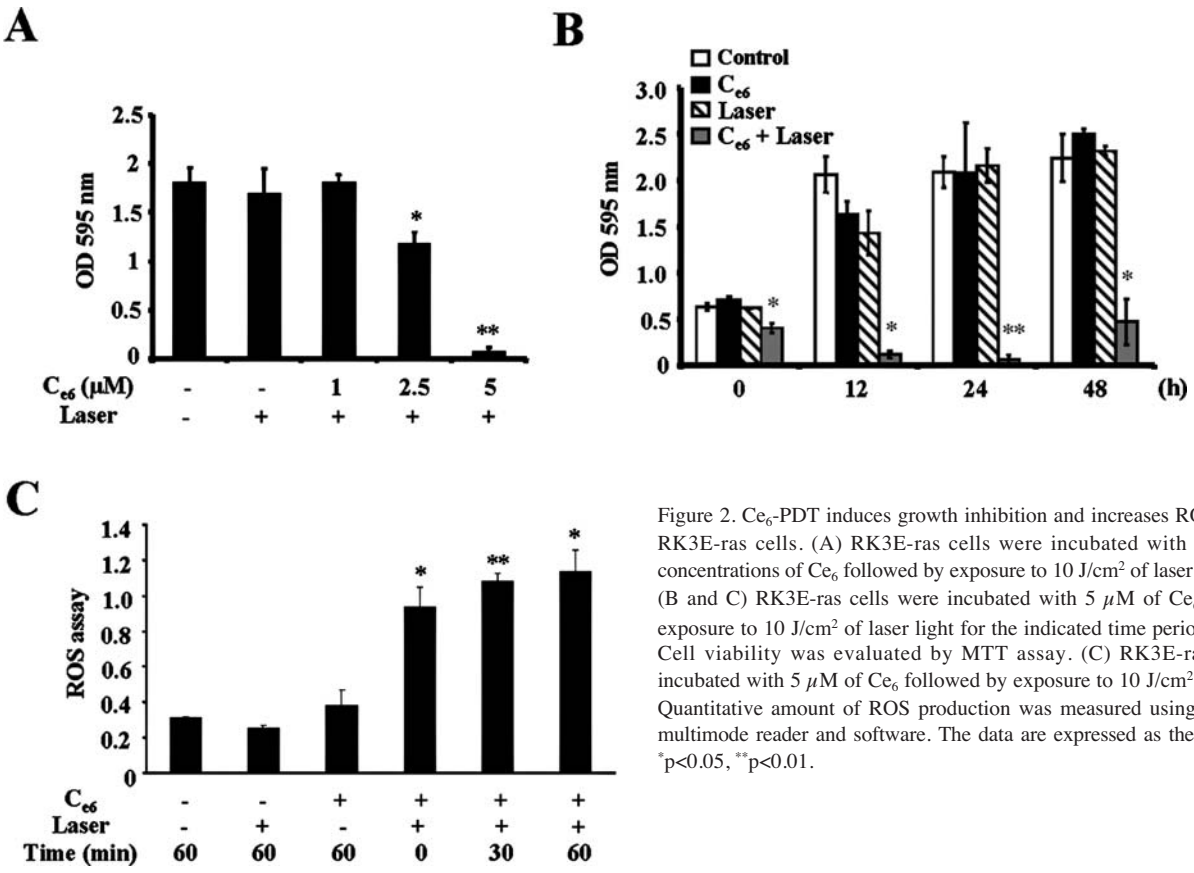

Figure 2. Ce_6-PDT induces growth inhibition and increases ROS content on RK3E-ras cells. (A) RK3E-ras cells were incubated with the indicated concentrations of Ce_6 followed by exposure to 10 J/cm^2 of laser light for 24 h. (B and C) RK3E-ras cells were incubated with 5 μM of Ce_6 followed by exposure to 10 J/cm^2 of laser light for the indicated time periods. (A and B) Cell viability was evaluated by MTT assay. (C) RK3E-ras cells were incubated with 5 μM of Ce_6 followed by exposure to 10 J/cm^2 of laser light. Quantitative amount of ROS production was measured using the scanning multimode reader and software. The data are expressed as the means ± SD. $^*p<0.05$, $^{**}p<0.01$.

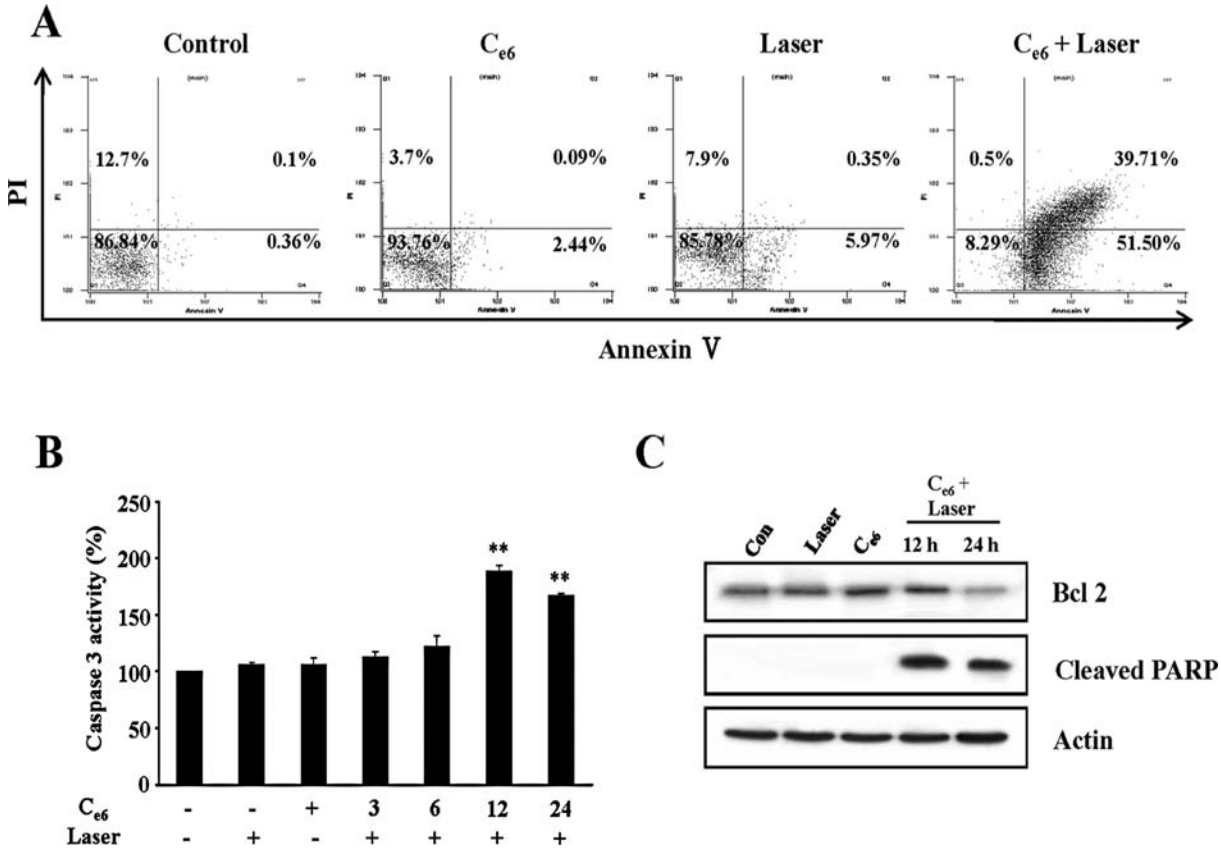

Figure 3. Ce_6-PDT induces the apoptosis through caspase-3 activation in RK3E-ras cells. RK3E-ras cells were incubated with 5 μM of Ce_6 for 24 h followed by exposure to 10 J/cm^2 of laser light. (A) Apoptosis was evaluated by the flow cytometric method by staining the cells with Annexin-V-FLUOS and propidium iodide. (B) Cells were lysed and caspase-3 activity was measured as described in Materials and methods. (C) The protein fraction was prepared and resolved by 12% SDS-PAGE. The expression levels of bcl-2, cleaved PARP, and actin were detected by Western blot analysis. $^{**}p<0.01$.

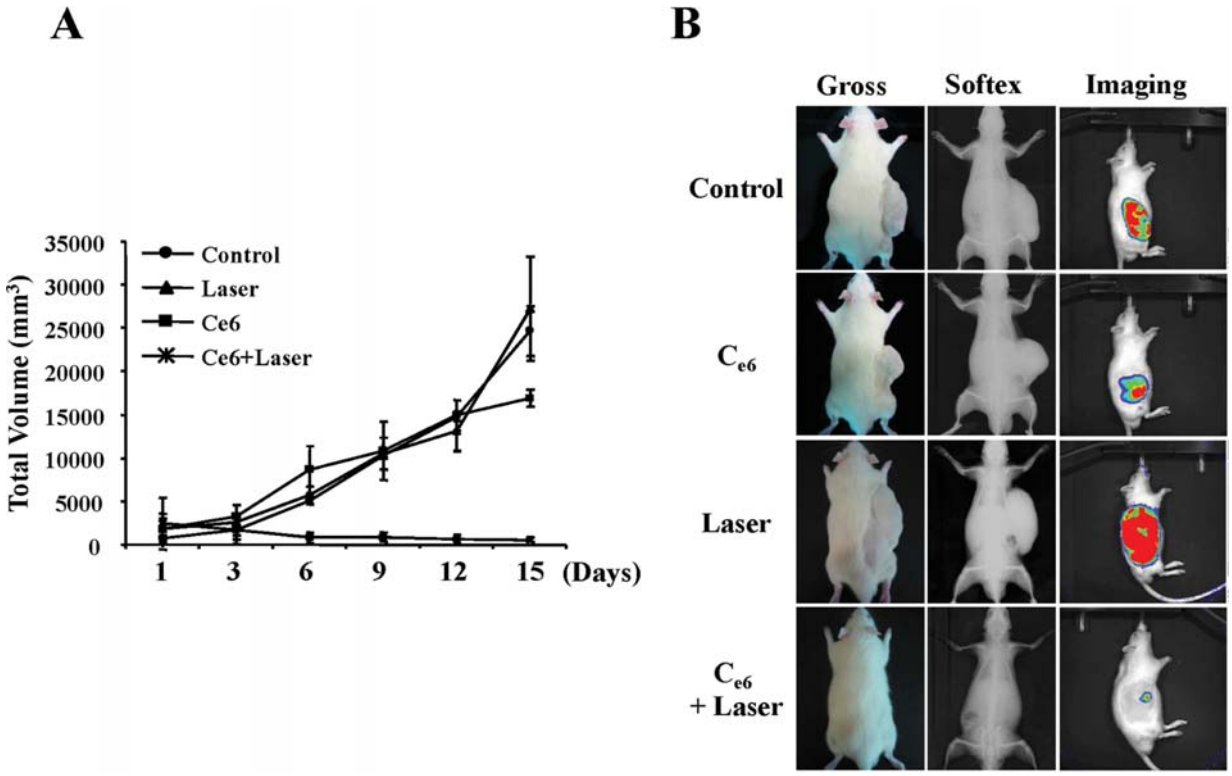

Figure 4. Ce_6-PDT inhibits tumor growth *in vivo*. RK3E-ras cells ($5x10^6$/rat) were injected s.c. into the right flank of SD rats. (A) Tumor volume was measured every 3 days and calculated using the formula $V=(ab^2)/2$, in which *a* is the largest diameter and *b* is the shortest diameter of the tumor. Results are expressed as mean ± SD. (B) Gross (left), soft X-ray imaging (middle), and *in vivo* bioluminescence images (right) obtained on day 15 after Ce_6-PDT.

chlorella, a key rich source of the starting material chlorophyll *a*.

The cytotoxic effect of PDT on the survival of Ce_6-treated cells was examined in a time- and dose-dependent manner using MTT assays. The viability of RK3E-ras cells was decreased by Ce_6-PDT depending on Ce_6 concentration (Fig. 2A). When Ce_6 was treated for 12 and 24 h, PDT most effectively reduced cell viability (Fig. 2B). The excited photosensitizer interacts with molecular oxygen and results in the production of ROS, which can lead to damage of the cellular constituents and subsequent cell destruction (12-14). It is believed that ROS plays a direct role in damaging cells subjected to PDT (2,4). Therefore, we examined intracellular ROS production by Ce_6-PDT in the RK3E-ras cells. ROS generation was induced immediately after Ce_6-PDT and increased in a time-dependent manner (Fig. 2C).

Apoptosis is responsible for PDT-mediated tumor inhibition in certain cell lines (15,16). To examine whether the growth-inhibitory effect of Ce_6-PDT in RK3E-ras cells is caused by apoptosis, flow cytometry was performed 24 h after Ce_6-PDT. Among Ce_6-PDT-treated cells, 51.5% cells were shown to be apoptotic and 39.71% is necrotic or late apoptotic (Fig. 3A).

Although cell death can be induced by PDT with different photosensitizers, the molecular characteristics involved in each death event might be different (14,17). To examine the molecular changes associated with cell death in RK3E-ras cells by Ce_6-PDT, we investigated caspase-3 activity, which is a hallmark of apotosis. Ce_6-PDT enhanced caspase-3 activity in a time-dependent manner (Fig. 3B), implicating that Ce_6-PDT triggers caspase-3 activation in RK3E-ras cells. Particularly, 12 h after PDT, caspase-3 activity showed an 88.6% increase compared with those in control group.

Caspase-3 plays an important role in the execution of apoptosis and is primarily responsible for the cleavage of PARP during cell death (18-22). The activation of PARP by DNA strand breaks contributes to the consumption of NAD and ATP that occurs in cells undergoing apoptosis (23,24). In this study, the cleavage of PARP was detected in Rk3E-ras cells 12 and 24 h after Ce_6-PDT (Fig. 3C). Moreover, the protein level of anti-apoptotic bcl-2 was reduced 24 h after Ce_6-PDT (Fig. 3C). These findings suggest that Ce_6-PDT might induce growth inhibition in RK3E-ras cells through apoptosis.

We previously demonstrated an animal model for rapid induction of malignant tumor (25). This animal model has the advantage of allowing short-term screening of antitumor agents. We examined the effect of Ce_6-PDT on *in vivo* tumor growth using this rat model with subcutaneous injection of RK3E-ras cells. Tumor volume was measured every three days after Ce_6-PDT and the results showed that Ce_6-PDT treatment arrested tumor progression (Fig. 4A). On gross, Softex X-ray, and bioluminescence images, the tumor almost disappeared in the rats treated with Ce_6-PDT (Fig. 4B). These results suggest that only a single application of Ce_6-PDT can inhibit effectively the progression of a solid tumor *in vivo*.

Histology of control tumors demonstrated solid growth of anaplastic undifferentiated carcinoma showing many mitotic figures with hemorrhage. However, Ce_6-PDT treatment led to

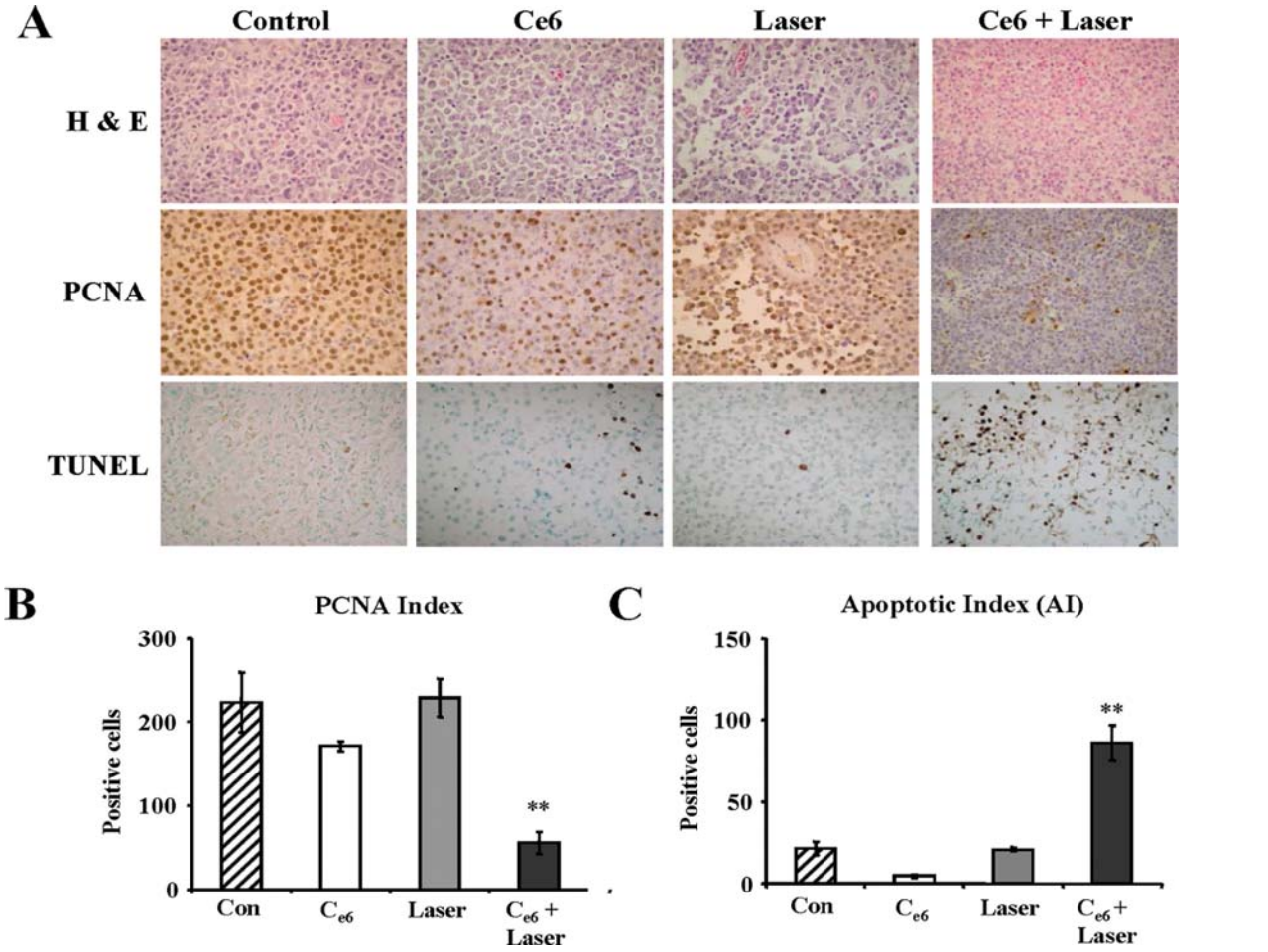

Figure 5. Ce_6-PDT decreases the proliferation and induces apoptosis of the tumor *in vivo*. (A) H&E staining of tumor sections (top), immunohistochemistry for PCNA (middle), and TUNEL assay (bottom) were performed on paraffin sections from tumor. (B) Positive cells for PCNA immunostaining (left) and (C) TUNEL (right) were counted and results are expressed as mean ± SD. $^{**}p<0.01$

loss of cohesiveness and extensive cell death showing nuclear pyknosis and cytoplasmic eosinophilia (Fig. 5A, top). Most of tumor cells in the control and treated with Ce_6 or laser alone were PCNA-positive, suggesting a high proliferative rate. However, the number of PCNA-positive cells significantly decreased in tumor treated with Ce_6-PDT (Fig. 5A and B). We also performed TUNEL staining to assess the amount of the apoptotic cells *in vivo*. TUNEL-positive cells significantly increased in tumor treated with Ce_6-PDT compared with the control untreated (Fig. 5A and C). These results confirmed *in vitro* data that Ce_6-PDT effectively arrested the tumor growth by inhibiting cell proliferation and inducing apoptosis.

In summary, we showed herein that PDT using newly purified second-generation photosensitizer Ce_6 exerted cytotoxic effect via the intracellular ROS production on the RK3E-ras cell line that induces rapid malignant tumor growth in SD rats. Ce_6-PDT also induced apoptosis through the activation of caspase-3, and its downstream target, PARP cleavage. In addition, Ce_6-PDT effectively arrested the tumor growth by inhibiting cell proliferation and inducing apoptosis. Therefore, the present study suggests that the newly purified Ce_6-PDT may be useful in the clinical application to control solid tumors.

Acknowledgements

This work was supported by grant No. BPF-2007-R04 from the Regional Technology Innovation Program of the Ministry of Commerce, Industry and Energy (MOCIE) and KOSEF/MOST (R13-2008-010-01001-0).

References

1. Frimberger AE, Moore AS, Cincotta L, Cotter SM and Foley JW: Photodynamic therapy of naturally occurring tumors in animals using a novel benzophenothiazine photosensitizer. Clin Cancer Res 4: 2207-2218, 1998.
2. Dolmans DE, Fukumura D and Jain RK: Photodynamic therapy for cancer. Nat Rev Cancer 3: 380-387, 2003.
3. Lu Z, Tao Y, Zhou Z, *et al*: Mitochondrial reactive oxygen species and nitric oxide-mediated cancer cell apoptosis in 2-butylamino-2-demethoxyhypocrellin B photodynamic treatment. Free Radic Biol Med 41: 1590-1605, 2006.
4. Gomer CJ, Ferrario A, Luna M, Rucker N and Wong S: Photodynamic therapy: combined modality approaches targeting the tumor microenvironment. Lasers Surg Med 38: 516-521, 2006.
5. Moan J and Berg K: Photochemotherapy of cancer: experimental research. Photochem Photobiol 55: 931-948, 1992.
6. Roberts WG, Shiau FY, Nelson JS, Smith KM and Berns MW: In vitro characterization of monoaspartyl chlorin e6 and diaspartyl chlorin e6 for photodynamic therapy. J Natl Cancer Inst 80: 330-336, 1988.

7. Isakau HA, Trukhacheva TV, Zhebentyaev AI and Petrov PT: HPLC study of chlorin e6 and its molecular complex with polyvinylpyrrolidone. Biomed Chromatogr 21: 318-325, 2007.
8. Isakau HA, Trukhacheva TV and Petrov PT: Isolation and identification of impurities in chlorin e6. J Pharm Biomed Anal 45: 20-29, 2007.
9. Kolligs FT, Hu G, Dang CV and Fearon ER: Neoplastic transformation of RK3E by mutant beta-catenin requires deregulation of Tcf/Lef transcription but not activation of c-myc expression. Mol Cell Biol 19: 5696-5706, 1999.
10. Kim SA, Kim YC, Kim SW, *et al*: Antitumor activity of novel indirubin derivatives in rat tumor model. Clin Cancer Res 13: 253-259, 2007.
11. Carlsson G, Gullberg B and Hafstrom L: Estimation of liver tumor volume using different formulas - an experimental study in rats. J Cancer Res Clin Oncol 105: 20-23, 1983.
12. Girotti AW: Photodynamic lipid peroxidation in biological systems. Photochem Photobiol 51: 497-509, 1990.
13. Henderson BW and Dougherty TJ: How does photodynamic therapy work? Photochem Photobiol 55: 145-157, 1992.
14. Hsieh YJ, Wu CC, Chang CJ and Yu JS: Subcellular localization of Photofrin determines the death phenotype of human epidermoid carcinoma A431 cells triggered by photodynamic therapy: when plasma membranes are the main targets. J Cell Physiol 194: 363-375, 2003.
15. Agarwal ML, Clay ME, Harvey EJ, Evans HH, Antunez AR and Oleinick NL: Photodynamic therapy induces rapid cell death by apoptosis in L5178Y mouse lymphoma cells. Cancer Res 51: 5993-5996, 1991.
16. Granville DJ, Carthy CM, Jiang H, Shore GC, McManus BM and Hunt DW: Rapid cytochrome c release, activation of caspases 3, 6, 7 and 8 followed by Bap31 cleavage in HeLa cells treated with photodynamic therapy. FEBS Lett 437: 5-10, 1998.
17. Yang J, Liu X, Bhalla K, *et al*: Prevention of apoptosis by Bcl-2: release of cytochrome c from mitochondria blocked. Science 275: 1129-1132, 1997.
18. Alnemri ES, Livingston DJ, Nicholson DW, *et al*: Human ICE/CED-3 protease nomenclature. Cell 87: 171, 1996.
19. Cryns V and Yuan J: Proteases to die for. Genes Dev 12: 1551-1570, 1998.
20. Le Rhun Y, Kirkland JB and Shah GM: Cellular responses to DNA damage in the absence of Poly(ADP-ribose) polymerase. Biochem Biophys Res Commun 245: 1-10, 1998.
21. Nicholson DW, Ali A, Thornberry NA, *et al*: Identification and inhibition of the ICE/CED-3 protease necessary for mammalian apoptosis. Nature 376: 37-43, 1995.
22. Tewari M, Quan LT, O'Rourke K, *et al*: Yama/CPP32 beta, a mammalian homolog of CED-3, is a CrmA-inhibitable protease that cleaves the death substrate poly(ADP-ribose) polymerase. Cell 81: 801-809, 1995.
23. Berger NA and Petzold SJ: Identification of minimal size requirements of DNA for activation of poly(ADP-ribose) polymerase. Biochemistry 24: 4352-4355, 1985.
24. Berger NA: Poly(ADP-ribose) in the cellular response to DNA damage. Radiat Res 101: 4-15, 1985.
25. Kim SA, Kim HW, Kim DK, *et al*: Rapid induction of malignant tumor in Sprague-Dawley rats by injection of RK3E-ras cells. Cancer Lett 235: 53-59, 2006.